pISSN : 1976-0620, eISSN : 2384-0633
https://doi.org/10.7742/jksr.2019.13.4.589 "J. Korean Soc. Radiol., Vol. 13, No. 4, August 2019"

The Study on Interpretation of the Scatter Degradation Factor using an additional Filter in a Medical Imaging System

Sang Sik Kang,[1] Kyo Tae Kim,[2] Ji Koon Park[1,*]

[1]Department of Radiological Science, International University of Korea
[2]Research Team of Radiological Physics & Engineering, Korea Institute of Radiological & Medical Sciences of Korea

Received: July 30, 2019. Revised: August 28, 2019. Accepted: August 31, 2019

ABSTRACT

X-rays used for diagnosis have a continuous energy distribution. However, photons with low energy not only reduce image contrast, but also contribute to the patient's radiation exposure. Therefore, clinics currently use filters made of aluminum. Such filters are advantageous because they can reduce the exposure of the patient to radiation. However, they may have negative effects on imaging quality, as they lead to increases in the scattered dose. In this study, we investigated the effects of the scattered dose generated by an aluminum filter on medical image quality. We used the relative standard deviation and the scatter degradation factor as evaluation indices, as they can be used to quantitatively express the decrease in the degree of contrast in imaging. We verified that the scattered dose generated by the increase in the thickness of the aluminum filter causes degradation of the quality of medical images.

Keywords: X-ray, image quality, aluminum filter, scatter degradation factor

I. INTRODUCTION

Diagnostic radiation generators are currently widely used in the clinic. These devices are used to acquire medical images using X-rays with continuous energy distributions. Since a medical image is a contrast image acquired based on information regarding a patient's anatomical structure, object contrast is a very important factor in medical imaging. In recent years, safety regulations have been strengthened in response to growing demand for safety worldwide. In line with this global trend, various studies have been carried out to reduce patient exposure to radiation while improving the quality of medical images.[1,2] One technique used to achieve these goals in the use of additional filters to increase the average X-ray energy by lowering the ratio of low-energy photons, which are known to increase exposure to continuous X-rays; low-energy photons cannot contribute to medical imaging, as they cannot penetrate the body. For this reason, an Al filter that decreases the amount of low-energy photons is currently used in clinics, in order to reduce the patient's radiation dose. However, although X-ray beam-hardening increases the scattered radiation generated in objects and thereby elevates the ratio of the scattered radiation incident on a detector, research on this effect has been relatively insufficient. Therefore, this study investigated the effects of scattered dose created by thickness of various filters on medical imaging quality.

II. EXPERIMENTS

1. Experimental setup

* Corresponding Author: Ji Koon Park E-mail: radiopjk@iuk.ac.kr Tel: +82-55-751-8301
Address: 965 dongburo munsaneup jinju gyeongnam, korea

In this study, an Al filter, which is widely used in medical imaging systems, was installed in the bottom of a collimator. The national council on radiation protection and measurements (NCRP) recommends the use of the following filter thicknesses based on the magnitude of the X-ray energy: 0.5 mmAl for 50 kVp or less, 1.5 mmAl for 50 kVp to 70 kVp, and 2.5 mmAl for 70 kVp or higher.[3] In order to evaluate changes associated with the thickness of the Al filter, the thickness of the Al filter was varied from 0.0 mm to 2.5 mm. Additionally, we fabricated a chest phantom corresponding to a high frequency of radiological imaging using patient-equivalent materials to generate a scattered ray.

The phantom was designed based on the suggestions of the american national standards institute (ANSI), as shown in Fig. 1.

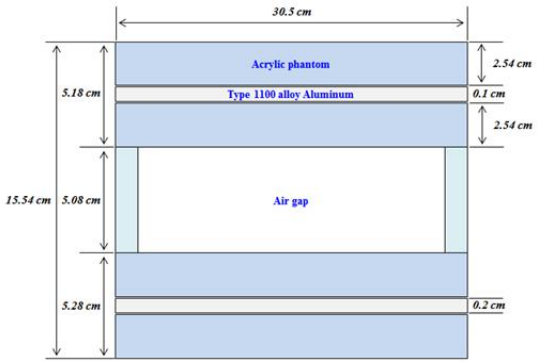

Fig. 1. Schematic diagram of the ANSI chest phantom.

The ANSI phantom comprised four identical acrylic sheets and two Al sheets with different thicknesses. The acrylic and Al phantoms were specifically designed by the manufacturer to conform to the recommendations of American Association of Physicists in Medicine Report No. 31.[4] Furthermore, to reproduce a lung filled with air, an air gap of 5.08 cm was left inside the phantom using four positioning rods. For the chest anteroposterior irradiation condition, we used average values of 85 kVp tube voltage and 7.5 mAs tube current, as reported by the korea food and drug administration.[5]

2. Analysis of forward scattering rate

In this study, after placing an ion chamber at the bottom of the ANSI phantom, as shown in Fig. 2, absorption doses were measured to evaluate the forward scattering rate (FSR). In these experiments, a 0.3-mmPb shield was positioned on top of the ANSI phantom as shown in Fig. 2(a) to block the primary radiation. The scattered dose was then measured. Based on information obtained using the x-ray dosemeter (XR-Sensor, IBA Dosimetry, Germany), FSR was calculated using the equation below[6]:

$$FSR(\%) = I_S \times I_T^{-1} \times 100 \quad (1)$$

where I_S the scattered radiation intensity and I_T is the total radiation intensity.

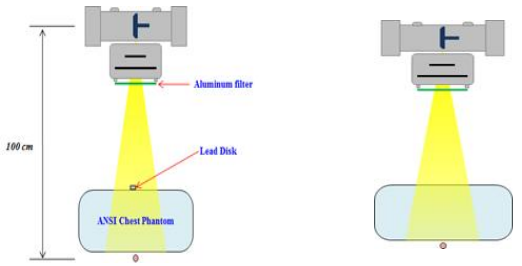

(A) Scattered radiation (B) Total radiation

Fig. 2. Schematic diagram of the experiment setup for the measurement.

3. Analysis of scatter degradation factor

In this study, we used the scatter degradation factor (SDF) as a quantitative evaluation index of operational degradation in medical imaging due to the scattered dose generated by the filters. The SDF is a value less than unity, with smaller values indicating a greater reduction in contrast due to scatter.[7] SDF was calculated using the equation below:[8]

$$SDF = I_P \times (I_P + I_S)^{-1} \quad (2)$$

where I_P is the primary radiation intensity and I_S is the

scattered radiation intensity.

4. Analysis of relative standard deviation

We calculated the relative standard deviation (RSD) to analyze the effects of the increase in the scattered dose due to the increase in the thickness of the Al filter. A commercially available flat panel detector (FLAATZ 560, DRTech Co., Korea) was used to obtain the images and evaluate their quality in relation to the thickness of the Al filter. The FLAATZ 560 device comprises an array of 2,560 × 3,072 pixels with a pixel pitch of 139 μm. Image processing was performed using Octave software (Octave Ver. 4.0.2, Free Software Foundation Inc., USA). After the images were obtained, the pixel values of the flat panel detector-based X-ray dose were analyzed as raw data.

In order to quantitatively analyze the effects of the scattered dose, 10 X-ray images were acquired with and without an ANSI phantom. These images were then averaged. A 1,024 × 1,024 pixel array was used as an region of interest (ROI) to produce the images. RSD was then used as an evaluation index based on the obtained images; RSD is defined as the ratio of the standard deviation to the mean value of the pixels in the ROI. Generally, lower RSD values indicate smaller standard deviations, which are required to obtain uniform medical images. We calculated RSD using the following equation:

$$RSD = X_{Ave}^{-1} \times ((\sum(X_i - X_{Ave})^2) \times n^{-1})^{0.5} \quad (3)$$

where X_i is the value of each pixel, X_{Ave} is the average pixel value, and n is the number of pixels in the image.

5. Analysis of noise power spectrum

In this study, the noise power spectrum (NPS) was calculated to analyze the effects of the increase in the scattered dose due to the increase in the thickness of the Al filter. In order to quantitatively analyze the effects of the scattered dose, 8 X-ray images were acquired from an ANSI phantom and then averaged. In addition, 256 × 256 pixel arrays were used as an ROI to produce the two-dimensional NPS images. Normalized NPS was then used as an evaluation index based on the obtained images.

III. RESULT AND DISCUSSION

1. Analysis of FSR

FSR increased as a linear function of the thickness of the Al filter, as shown in Fig. 3. The FSR was 37.3% when using a 0 mmAl filter, 37.59% when using a 1.5 mmAl filter, and 37.79% when using a 2.5 mmAl filter. The coefficient of determination of the fit curve (denoted as R-Sq) was calculated based on the calculated FSR. We calculated an R-Sq value of 0.9928 and a fit curve with the following equation: Y_1=0.1914X + 37.317, where Y_1 is the FSR and X is the thickness of the Al filter. These results verified that the scattered dose increased as the thickness of filter increases, and confirmed the effects of X-ray beam hardening quantitatively.

The absorbed dose incident on the actual detector decreased exponentially, as shown in Fig. 3(a). The R-Sq of the fit curve for this trend was found to be 0.995. The fit curve had the following equation: $Y_2 = 0.804\ e^{-0.258}X$, where Y_2 denotes the absorbed dose. This result confirmed that the ratio of the scattered dose to the incident dose increases gradually as the filter becomes thicker. The SDF decreased as an inverse linear function of the thickness of the Al filter, as shown in Fig. 3(b). The R-Sq of the fit curve for this trend was found to be 0.9928. The fit curve had the following equation: $Y_3 = -0.0019X + 0.6268$, where Y_3 denotes the SDF. These results verified that functional degradation occurs in medical imaging as the scattered dose increases.

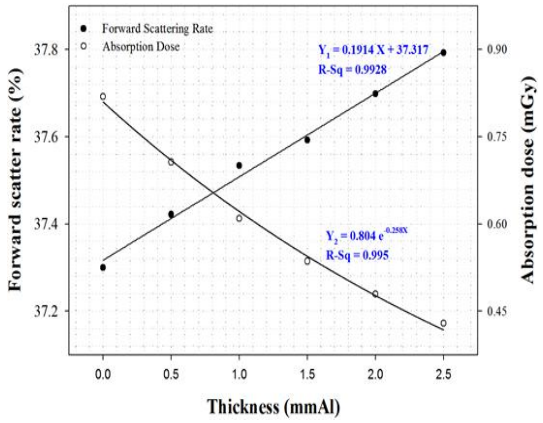

(a) Forward scatter rate (left) and absorption dose (right)

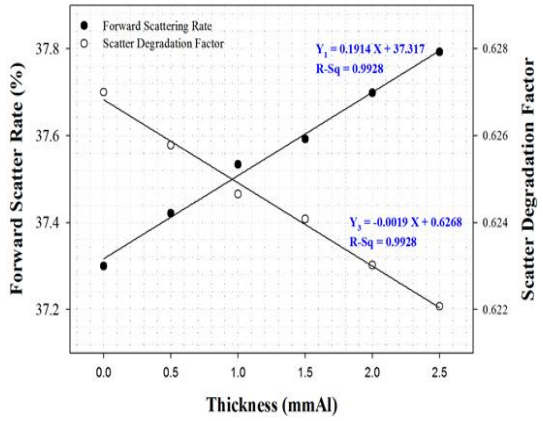

(b) Forward scatter rate (left) and scatter degradation factor (right)

Fig. 3. Scatter as a function of the thickness of the aluminum filter.

2. Radiographic effects

As shown in Fig. 4(a), the root mean square (RMS) image density was very uniform in the absence of the ANSI phantom. We did not use an ANSI phantom to generate the scattered dose. The data obtained using this approach is thus referred to as data "without scatter". As shown in Fig. 4(b), when the ANSI phantom was used, a round latent image appeared on the RMS image, and the image density was uneven throughout. The latent image is thought to be produced due to recoil electrons and scattered photons generated by the Compton scattering effect. The angular distributions of the recoil electrons and the scattered photons can be estimated using the Klein-Nishina equation, and their relationships can be explained using the following equation.[9]

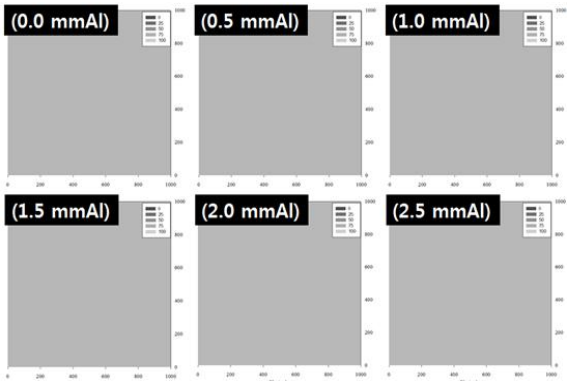

(a) Without ANSI chest phantom

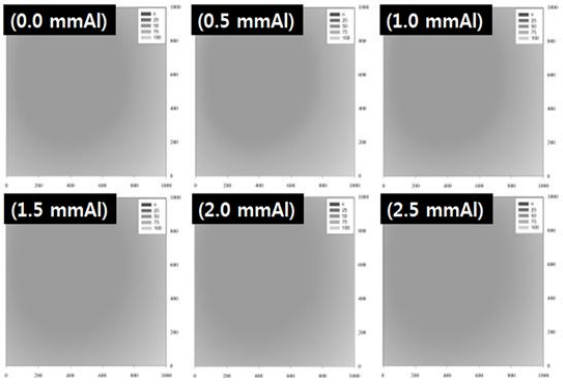

(b) With ANSI chest phantom

Fig. 4. Images classified according to the thickness of the aluminum filter used in the medical imaging system.

$$\cos\theta = 1 - 2 \times ((1 + \alpha)^2 \times \tan^2\varphi + 1)^{-1} \quad (4)$$

where θ is the angle of the Compton scattered photon, α is the unit photon energy of the electron rest mass energy, and φ is the angle of the recoil electron. Ultimately, higher energies of incident light lead to higher rates of forward scattering.[10] This observation may be explained by the FSR shown in Fig. 4. Our findings verified that the scattered dose generated by X-ray beam-hardening could affect medical images.

2.1 Analysis of RSD

The RSD was 0 regardless of the increase in the thickness of the filter when the ANSI phantom was absent, as seen in Fig. 5.

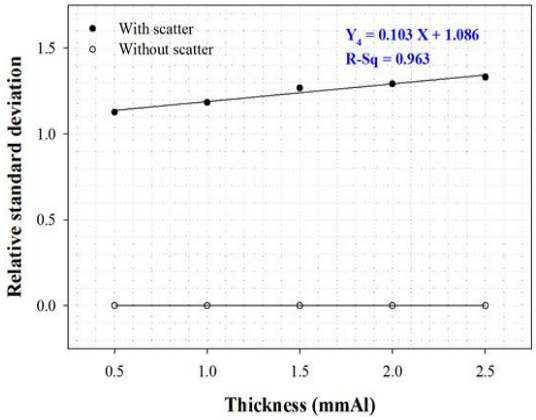

Fig. 5. Relative standard deviation as a function of the thickness of the filter.

The average value of the pixels was about 28 and remained constant. The standard deviation was 0. Based on these results, we quantitatively verified the qualitative evaluation that the RMS images had very uniform density, as seen in Fig. 4(a). When the ANSI phantom was used, the RSD value gradually increased with increasing filter thickness, as follows: 1.185 for 0 mmAl filter, 1.267 for 1.5 mmAl filter, and 1.33 for 2.5 mmAl filter. These results indicate that the forward scattering dose generated at the ANSI phantom by X-ray beam-hardening has a significant effect on medical images. We subsequently reconfirmed that the round latent image seen in Fig. 4(b) was affected by the forward scattering dose. We found an R-Sq value of 0.963 for the fit curve based on the calculated RSD value, which was obtained using the following equation: $Y_4 = 0.103\ X + 1.086$, where Y_4 denotes the RSD. Based on these results, we quantitatively verified the qualitative evaluation that the image was non-uniform overall due to the round latent image.

3. Evaluation of NPS

We averaged the data obtained from the 10 X-ray images. The NPS image indicating the noise components in the frequency space was drawn as shown in Fig. 6.

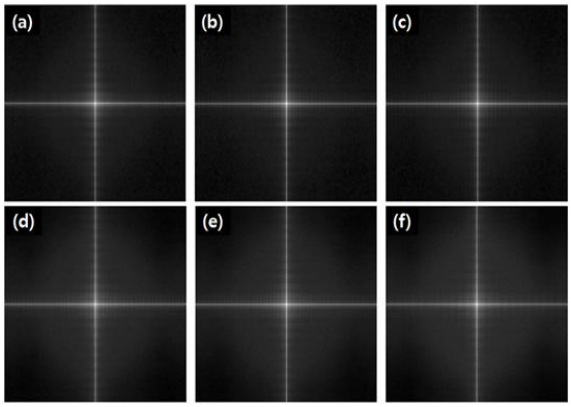

Fig. 6. Noise power spectra for images classified according to the thickness of the aluminum filter used in the medical imaging system. (a) 0 mmAl, (b) 0.5 mmAl, (c) 1.0 mmAl, (d) 1.5 mmAl, (e) 2.0 mmAl, and (f) 2.5 mmAl

The NPS image defines low-frequency noise when it approaches the origin and noise of high frequency when it is distant from the origin.[11,12] The normalized NPS was computed based on the obtained NPS image. The normalized NPS can be estimated based on the NPS profile (or 1D-NPS), gain (denoted G), and absorption dose (denoted X). The relationships among these parameters can be explained using the following equation:

$$NNPS = NPS(f) \times (G \times X)^2 \qquad (5)$$

where NNPS is the normalized NPS and NPS(f) is the NPS profile as a function of the spatial frequency. In this study, the value of X was obtained based on the graph in Fig. 3(b) and the value of G was 1. X was measured in units of Gy. The NNPS gradually decreased as the spatial frequency increased, and steadily increased as the thickness of the Al filter increased.

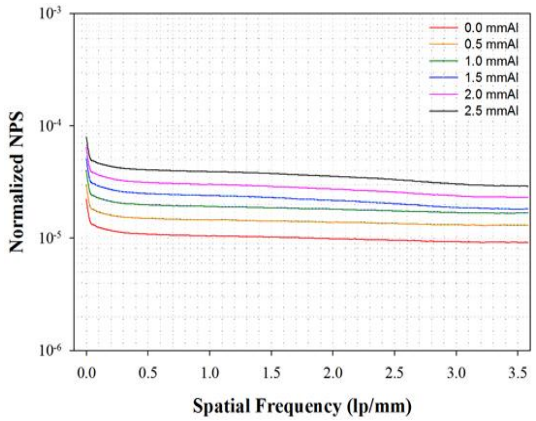

Fig. 7. Normalized noise power spectrum as a function of spatial frequency.

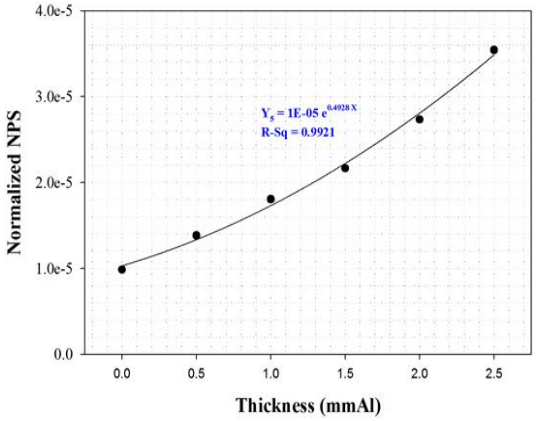

Fig. 8. Normalized noise power spectrum as a function of the thickness of the aluminum filter at 2.0 lp/mm.

For a more quantitative analysis, a spatial frequency of 2.0 lp/mm was used as a standard, as this evaluation index is a frequency close to the limit recognized by humans.[13] This analysis at 2.0 lp/mm yielded NNPS values of 9.85×10^{-6} at 0 mmAl, 2.17×10^{-5} at 1.5 mmAl, and 3.54×10^{-5} at 2.5 mmAl, as shown in Fig. 8. We found an R-Sq value of 0.9921 for the fit curve based on the calculated NNPS value from the limited frequency based on the following equation: $Y_5 = 1E\text{-}05\ e^{0.4928X}$, where Y_5 denotes the NNPS.

IV. CONCLUSION

Recently, due to increased demand for safety worldwide, a number of studies on additional X-ray filters used to reduce patient X-ray exposure have been carried out. However, the scattered dose increases with the addition of filters. This in turn may adversely affect medical images. This effect of additional filtering has not received much attention. Thus, we quantitatively verified that thicker additional filters lead to larger changes in the scattered dose due to X-ray beam-hardening and have greater effects on medical images.

The results of this study are consistent with the Klein-Nishina equation, which describes the probability of Compton scattering, which predominantly affects the generation of scattered radiation in the diagnostic radiation energy range. The Klein-Nishina equation indicates that incident light beams with higher energies lead to higher forward scattering rates. When we used a 2.5 mmAl filter, which is recommended for use with tube voltages of 70 kVp or higher by the NCRP, we observed a 0.69% change in FSR and a change of 0.146 in RSD when compared to the condition wherein the filter was not used. In addition, there was a difference of 0.005 in SDF and of 3.59 mm^2 in NNPS.

Considering that medical imaging relies on the degree of X-ray absorption as a contrast for a given subject configuration, the result of a decrease in SDF is highly significant, because this indicates that imaging contrast is diminished by the scattered dose. Thus, we quantitatively verified that the scattered dose increases noise in medical images and adversely affects image quality depending on the thickness of the additional filter. It is expected that these results are used as a basis for future filter research in order to improve image quality.

Acknowledgement

This work was supported by a National Research Foundation of Korea (NRF) grant funded by the Korean government (MSIP)

(No. 2017R1A2B4009249).

Reference

[1] World Health Organization, "International basic safety standards for protection against ionizing radiation and for the safety of radiation sources," International Atomic Energy Agency, Vienna, 1996.

[2] J. Valentin, "The 2007 recommendations of the international commission on radiological protection," Elsevier, Oxford, 2007.

[3] R. O. Gorson, "NCRP 33: Medical X-ray and gamma ray protection for energies up to 10 MeV-Equipment design and use," National Council on Radiation Protection and Measurements, Washington, D.C., 1968.

[4] R. Y. L. Chu and J. Fisher, "Standardized methods for measuring diagnostic x-ray exposures," American Institute of Physics, New York, 1990.

[5] G. H. Lee, "Normal scan of the patient dose recommendation amount of radiology guidelines," Korea Food and Drug Administration, Cheongju, 2012.

[6] I. H. Choi, K. T. Kim, Y. J. Heo, S. S. Kang, S. C. Noh, B. J. Jung, S. H. Nam, J. K. Park, "The study of forward scattering dose according to the thickness of filter in general radiography," Journal of the Korean Society of Radiology, Vol. 9, No. 7, pp. 445-448, 2015.

[7] G. Dougherty, "Digital image processing for medical applications," Cambridge University Press, New York, 2009.

[8] H. Aichinger, J. Dierker, S. J. Barfuß, M. Säbel, "Radiation exposure and image quality in X-ray diagnostic radiology," Springer, Heidelberg, 2012.

[9] C. M. Davisson and R. D. Evans, "Gamma-Ray absorption coefficients," Reviews of Modern Physics, Vol. 24, No. 2, pp. 79-107, 1952.

[10] R. D. Evans and N. Atome, "The Atomic Nucleus," McGraw-Hill, New York, 1955.

[11] J. H. Siewerdsen, L. E. Antonuk, Y. E. Mohri, J. Yorkston, W. Huang, I. A. Cunningham, "Signal, noise power spectrum, and detective quantum efficiency of indirect-detection flat-panel imagers for diagnostic radiology," Medical Physics, Vol. 25, No. 5, pp. 614-628, 1998.

[12] L. Lanca and A. Silva, "Digital radiography detectors–A technical overview: Part 2," Radiography, Vol. 15, No. pp. 134-138, 2009.

[13] C. B. Kim, "The MTF measurement of the conventional x-ray system by using the computed radiography," Journal of the Korean Society of Radiology Sciences, Vol. 28, No. 2, pp. 111-115, 2005.

의료 영상 시스템에서 부가 필터를 이용한 산란 열화 인자의 해석에 관한 연구

강상식,[1] 김교태,[2] 박지군[1,*]

[1]한국국제대학교 방사선학과
[2]한국원자력의학원 의학물리공학연구팀

요 약

진단방사선 영상을 획득하기 위해 이용되는 X-ray는 연속적인 에너지 분포를 가지지만 저에너지 광자의 경우에는 영상 형성 보다는 환자피폭에 더 많은 기여를 하는 것으로 알려져 있다. 이러한 저에너지 광자를 제거하기 위해 임상에서는 알루미늄 필터를 적용하고 있으나 이는 빔 경화 현상으로 인한 영상 품질에 악영향을 미칠 가능성이 있다. 이에 본 연구에서는 알루미늄 필터에 의한 산란 선량이 의료 영상의 품질에 미치는 영향에 대하여 고찰하고자 하였다. 또한, 영상의 대조도 저하를 정량적으로 표현하기 위해 상대 표준 편차 및 산란 열화 인자를 평가 지표로서 활용하였다. 연구 결과, 70 kVp 이상의 전압에서 진단 영상을 확보 시 NCRP에 의해 권장되는 2.5 mmAl를 기준에서 전방산란율 분석 결과 0.69 %, 산란 열화 인자 분석 결과는 0.005, NNPS 분석 결과 3.59 mm2의 변화가 나타났다. 이러한 연구 결과를 바탕으로 알루미늄 필터의 두께가 증가함에 따라 발생하는 산란 선량이 의료 영상의 품질을 저하시키는 것을 정량적으로 검증하였다.

중심단어: 엑스선, 화질, 알루미늄 필터, 산란 열화 인자

연구자 정보 이력

	성명	소속	직위
(제1저자)	강상식	한국국제대학교 방사선학과	교수
(공동저자)	김교태	한국원자력의학원 의학물리공학연구팀	연구원
(교신저자)	박지군	한국국제대학교 방사선학과	교수